Initial Energy Density of Gluons Produced in Very-High-Energy Nuclear Collisions

Alex Krasnitz
UCEH, Universidade do Algarve, Campus de Gambelas, P-8000 Faro, Portugal

Raju Venugopalan
Physics Department, Brookhaven National Laboratory, Upton, New York 11973
(Received 14 September 1999)

In very-high-energy nuclear collisions, the initial energy of produced gluons per unit area per unit rapidity, $(dE/L^2)/d\eta$, is equal to $f(g^2\mu L)(g^2\mu)^3/g^2$, where μ^2 is proportional to the gluon density per unit area of the colliding nuclei. For an SU(2) gauge theory, a nonperturbative computation of $f(g^2\mu L)$ shows that it varies rapidly for small $g^2\mu L$ but varies only by ~25%, from 0.208 ± 0.004 to 0.257 ± 0.005, for a wide range 35.36–296.98 in $g^2\mu L$. This includes the range relevant for collisions at the Relativistic Heavy Ion Collider (RHIC) and the Large Hadron Collider (LHC). Extrapolating to SU(3), we estimate $dE/d\eta$ for Au-Au collisions in the central region at RHIC and LHC.

PACS numbers: 24.85.+p, 12.38.Mh, 25.75.–q

The Relativistic Heavy Ion Collider (RHIC) at BNL will soon collide beams of Au ions at $\sqrt{s} = 200$ GeV/nucleon. Some years later, the Large Hadron Collider (LHC) at CERN will collide heavy ions at $\sqrt{s} \approx 5.5$ TeV/nucleon. The objective of these experiments is to understand the properties of very hot and dense partonic matter in QCD. It is of considerable interest to determine whether this hot and dense matter equilibrates to briefly form a plasma of quarks and gluons [1].

The dynamical evolution of such a system clearly depends on the initial conditions, namely, the parton distributions in the nuclei prior to the collision. For partons with transverse momenta $p_t \gg \Lambda_{\rm QCD}$, cross sections in the standard perturbative QCD approach may be computed by convolving the parton distributions of the two nuclei with the elementary parton-parton scattering cross sections. At the high energies of RHIC (LHC), hundreds (thousands) of minijets with p_t's of the order of several GeV may be formed [2]. Final state interactions of these minijets are often described in multiple scattering or in classical cascade approaches [3]. Estimates for the initial energy density in a self-screened parton cascade approach can be found in Ref. [4].

At central rapidities, where $x \ll 1$, and $p_t \gg \Lambda_{\rm QCD}$ with x defined to be $p_t/\sqrt{s}$, parton distributions grow rapidly, and may even saturate for large nuclei for x's in the range 10^{-2} to 10^{-3} relevant for nuclear collisions at RHIC and LHC, respectively [5]. Coherence effects are important here, and are included only heuristically in the above-mentioned perturbative approaches.

In this Letter, we will describe results from a classical effective field theory (EFT) approach which includes coherent effects in the small x parton distributions of large nuclei [6]. If the parton density in the colliding nuclei is large at small x, classical methods are applicable. It has been shown recently that a renormalization group improved generalization of this effective action reproduces several key results in small x QCD: the leading $\alpha_S \log(1/x)$ Balitskii-Fadin-Kuraev-Lipatov equation, the double log Gribov-Levin-Ryskin equation and its extensions, and the small x Dokshitzer-Gribov-Lipatov-Altarelli-Parisi equation for quark distributions [7,8].

The EFT contains one dimensionful parameter μ^2, which is the variance of a Gaussian weight over the color charges $\rho^\pm$ of partons, of each nucleus, at rapidities higher than the rapidity of interest. For central impact parameters, it is determined to be [9]

$$\mu^2 = \frac{A^{1/3}}{\pi r_0^2}\int_{x_0}^{1} dx\left(\frac{1}{2N_c}\, q(x,Q^2) + \frac{N_c}{N_c^2-1}\, g(x,Q^2)\right), \tag{1}$$

where $xq(x,Q^2)$ and $xg(x,Q^2)$ stand for the *nucleon* quark and gluon structure functions at the resolution scale Q of the physical process of interest. Also, one has $x_0 = Q/\sqrt{s}$, $r_0 = 1.12$ fm, and N_c is the number of colors. From the Hadron Electron Ring Accelerator data for q and g, one obtains $\mu \le 1$ GeV for LHC energies and $\mu \le 0.5$ GeV at RHIC [9]. The classical gauge fields, and, hence, the classical parton distributions, can be determined analytically [7,10]. On this basis, it has been argued recently that the typical transverse momenta scale Q_s in this model is further in the weak coupling regime, with $Q_s \sim 1$ GeV for RHIC and $Q_s \sim 2$–3 GeV at LHC [11].

Kovner, McLerran, and Weigert [12] applied the effective action approach to nuclear collisions. (For an interesting alternative approach, see Ref. [13].) Assuming boost invariance, and matching the equations of motion in the forward and backward light cone, they obtained the following initial conditions for the gauge fields in the $A^\tau = 0$ gauge: $A_\perp^i|_{\tau=0} = A_1^i + A_2^i$, and $A^\pm|_{\tau=0} = \pm\frac{ig}{2}x^\pm[A_1^i, A_2^i]$. Here, $A_{1,2}^i(\rho^\pm)$ ($i = 1,2$) are the pure gauge transverse gauge fields corresponding to small x modes of incoming nuclei [with light cone sources

$\rho^{\pm}\delta(x^{\mp})]$ in the $\theta(\pm x^-)\theta(\mp x^+)$ regions, respectively, of the light cone.

The sum of two pure gauges in QCD is not a pure gauge—the initial conditions therefore give rise to classical gluon radiation in the forward light cone. For $p_t \gg \alpha_S\mu$, the Yang-Mills equations may be solved perturbatively to quadratic order in $\alpha_S\mu/p_t$. After averaging over the Gaussian random sources of color charge $\rho^{\pm}$ on the light cone, the perturbative energy and number distributions of physical gluons were computed by several authors [9,12,14], and shown, in the small x limit, to agree with the well-known quantum bremsstrahlung result [15].

In Ref. [16], we suggested a lattice discretization of the classical EFT, suitable for a nonperturbative numerical solution. Assuming boost invariance, we showed that, in $A^\tau = 0$ gauge, the real time evolution of the small x gauge fields $A_\perp(x_t,\tau), A^\eta(x_t,\tau)$ is described by the Kogut-Susskind Hamiltonian in $2+1$ dimensions coupled to an adjoint scalar field. The lattice equations of motion for the fields are then determined straightforwardly by computing the Poisson brackets. The initial conditions for the evolution are provided by the lattice analog of the continuum relations discussed earlier in the text. We impose periodic boundary conditions on an $N \times N$ transverse lattice, where N denotes the number of sites. The physical linear size of the system is $L = aN$, where a is the lattice spacing. It was shown in Ref. [17] that numerical computations on a transverse lattice agreed with lattice perturbation theory at large transverse momentum. For the numerical procedure, and other details, we refer the reader to Ref. [17].

In this Letter, we will focus on computing the energy density ε as a function of the proper time τ. Our main result is contained in Eq. (2). To obtain this result, we compute the Hamiltonian density on the lattice for each $\rho^{\pm}$, and then take the Gaussian average (with the weight μ^2) over between 40 ρ trajectories for the larger lattices and 160 ρ trajectories for the smallest ones.

In our numerical simulations, all the relevant physical information is compressed in $g^2\mu$ and L, and in their dimensionless product $g^2\mu L$ [18]. The strong coupling constant g depends on the hard scale of interest; from Eq. (1), we see that μ depends on the nuclear size, the center-of-mass energy, and the hard scale of interest; L^2 is the transverse area of the nucleus [19]. Assuming $g = 2$ (or $\alpha_S = 1/\pi$), $\mu = 0.5$ GeV (1.0 GeV) for RHIC (LHC), and $L = 11.6$ fm for Au nuclei, we find $g^2\mu L \approx 120$ for RHIC and $\approx$240 for LHC. (The latter number would be smaller for a smaller value of g at the typical LHC momentum scale.) As will be discussed later, these values of $g^2\mu L$ correspond to a region in which one expects large nonperturbative contributions from a sum to all orders in $\sim 6\alpha_S\mu/p_t$, even if $\alpha_S \ll 1$.

In Fig. 1, we plot $\varepsilon\tau/(g^2\mu)^3$, as a function of $g^2\mu\tau$, in dimensionless units, for the smallest, largest, and an intermediate value in the range of $g^2\mu L$'s studied. The quantity $\varepsilon\tau$ has the physical interpretation of the energy density of produced gluons $(dE/L^2)/d\eta$ only at late times—when $\tau \sim t$. Though $\varepsilon\tau$ goes to a constant in all three cases, the approach to the asymptotic value is different. For the smallest $g^2\mu L$, $\varepsilon\tau$ increases continuously before saturating at late times. Gluon distributions here are well defined when $k_t\tau \gg 1$ (see Ref. [12])—we expect saturation to occur when $\tau \gg L/2\pi$ and, indeed, that seems to be the case.

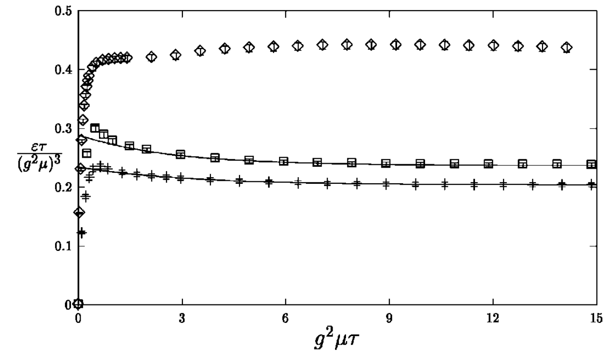

FIG. 1. $\varepsilon\tau/(g^2\mu)^3$ as a function of $g^2\mu\tau$ for $g^2\mu L = 5.66$ (diamonds), 35.36 (plusses), and 296.98 (squares). Both axes are in dimensionless units. Note that $\varepsilon\tau = 0$ at $\tau = 0$ for all $g^2\mu L$. The lines are exponential fits $\alpha + \beta e^{-\gamma\tau}$ including all points beyond the peak.

For larger values of $g^2\mu L$, $\varepsilon\tau$ increases rapidly, develops a transient peak at $\tau \sim 1/g^2\mu$, and decays exponentially there onwards, satisfying the relation $\alpha + \beta e^{-\gamma\tau}$, to a constant value α [equal to the lattice $(dE/L^2)/d\eta$]. The lines shown in the figure are from an exponential fit including all the points past the peak. This behavior is satisfied for all $g^2\mu L \geq 8.84$, independently of N. Given the excellent exponential fit, one can interpret the decay time $\tau_D = (1/\gamma)/g^2\mu$ as the appropriate scale controlling the formation of gluons with a physically well-defined energy. In other words, τ_D is the "formation time"in the sense used by Bjorken [20,21]. In Table I, we tabulate γ versus $g^2\mu L$ for the largest $N \times N$ lattices [22] for all but the smallest $g^2\mu L$. For large $g^2\mu L$, the formation time decreases with increasing $g^2\mu L$, as we expect it should.

In Fig. 2, we plot the asymptotic values α of $\varepsilon\tau/(g^2\mu)^3$ as a function of $g^2\mu a$ for various values of $g^2\mu L$. As shown in the upper part of Fig. 2, for smaller $g^2\mu L$, one can go very close to the continuum limit with excellent statistics (over 160 independent ρ trajectories for the two smallest values of $g^2\mu L$). In the lower part of Fig. 2, all the data give straight line fits with good χ-squared values. We use these fits to extrapolate the value of α in the continuum limit. We note that the largest value of $g^2\mu L$, with the smallest $g^2\mu a$ equal to 0.247, is relatively much further away from the continuum limit than the points in the upper part of the figure. It is obtained by averaging 40 independent trajectories on a 1200×1200 lattice. To lower $g^2\mu a$ below 0.1 would require going to lattices with 3000×3000 sites. This exceeds the CPU memory of our current computational resources. Nevertheless, even for

TABLE I. The function $f = (dE/L^2)/d\eta$ and the relaxation rate $\gamma = (1/\tau_D)/g^2\mu$ tabulated as a function of $g^2\mu L$. γ has no entry for the smallest $g^2\mu L$ since there $\varepsilon\tau/(g^2\mu)^3$ vs $g^2\mu\tau$ differs qualitatively from the other $g^2\mu L$ values.

$g^2\mu L$	5.66	8.84	17.68	35.36	70.7
f	0.436 ± 0.007	0.427 ± 0.004	0.323 ± 0.004	0.208 ± 0.004	0.200 ± 0.004
γ		0.101 ± 0.024	0.232 ± 0.046	0.165 ± 0.013	0.275 ± 0.011
$g^2\mu L$	106.06	148.49	212.13	296.98	
f	0.211 ± 0.004	0.232 ± 0.004	0.234 ± 0.007	0.257 ± 0.008	
γ	0.322 ± 0.012	0.362 ± 0.023	0.375 ± 0.038	0.378 ± 0.053	

the largest $g^2\mu L$, we do get a fine linear fit—though we would warn of a potentially large systematic error in the extrapolated value of $\varepsilon\tau/(g^2\mu)^3$.

The physical energy per unit area per unit rapidity of produced gluons can be defined in terms of a function $f(g^2\mu L)$ as

$$\frac{1}{L^2}\frac{dE}{d\eta} = \frac{1}{g^2} f(g^2\mu L)\,(g^2\mu)^3 \,. \tag{2}$$

The function f here is obtained by extrapolating the values in Fig. 2 to the continuum limit. In Fig. 3, we plot the striking behavior of f with $g^2\mu L$. For very small $g^2\mu L$'s, it changes very slightly but then changes rapidly by a factor of 2 from 0.427 to 0.208 when $g^2\mu L$ is changed from 8.84 to 35.36. From 35.36 to 296.98, nearly an order of magnitude in $g^2\mu L$, it changes by ~25%. The precise values of f and the errors are tabulated in Table I.

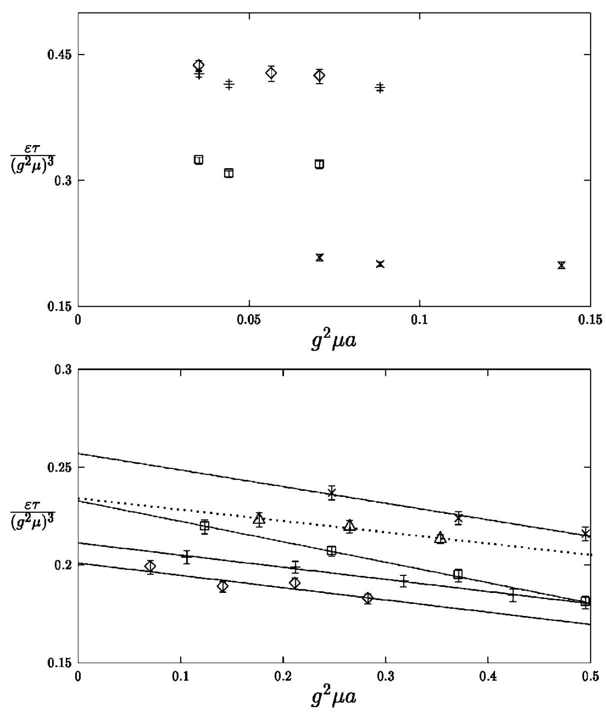

FIG. 2. $\varepsilon\tau/(g^2\mu)^3$ as a function of $g^2\mu a$. The points in the upper plot correspond to $g^2\mu L = 5.66$ (diamonds), 8.84 (plusses), 17.68 (squares), and 35.36 (×). The lower plot has $g^2\mu L = 70.7$ (diamonds), 106.06 (plusses), 148.49 (squares), 212.13 (triangles), and 296.98 (×). Lines in the lower plot are fits of form $a - b \times x$. The $g^2\mu a$ ranges are different in the two halves. The points in the upper half are typically closer to the continuum limit.

The dramatic change in the behavior of f as a function of $g^2\mu L$ can be traced to the initial conditions, namely, the parton distributions in the wavefunctions of the incoming nuclei [23]. In the nuclear wave function, at small x, nonperturbative, albeit weak coupling, effects become important for transverse momenta $Q_s \sim 6\alpha_s\mu$. The EFT predicts that classical parton distributions which have the characteristic Weizsäcker-Williams $1/p_t^2$ behavior for large transverse momenta ($p_t \gg Q_s$) grow only logarithmically for $p_t \leq Q_s$. One can therefore think of Q_s as a saturation scale [11] that tempers the growth of parton distributions at small momenta.

The saturation condition, $p_t \sim 6\alpha_S\mu$, roughly translates, on the lattice, into the requirement that $g^2\mu L \geq 13$ for the lowest momentum mode $n = 1$. Thus, for $g^2\mu L = 13$, one only begins to sample those modes. Indeed, this is the region in $g^2\mu L$ in which one sees the rapid change in f. The rapid decrease in f is likely because the first nonperturbative corrections are large, and have a negative sign relative to the leading term. Understanding the later slow rise and apparent saturation with $g^2\mu L$ requires a better understanding of the number and energy distributions with p_t [24].

Our results are consistent with an estimate by Mueller [25] for the number of produced gluons per unit area per unit rapidity. He obtains $(dN/L^2)/d\eta = c(N_c^2 - 1)Q_s^2/4\pi^2\alpha_S N_c$, and argues that the number c is a nonperturbative constant of order unity. If most of the gluons have

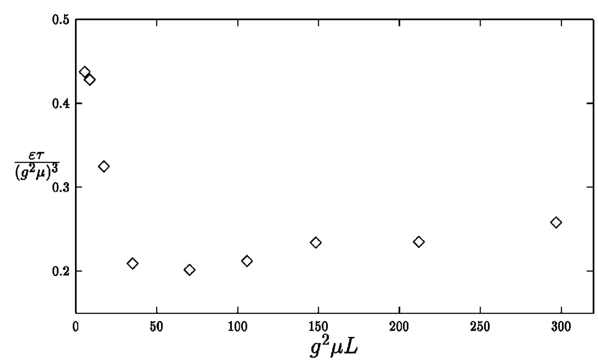

FIG. 3. $\varepsilon\tau/(g^2\mu)^3$ extrapolated to the continuum limit: f as a function of $g^2\mu L$. The error bars are smaller than the plotting symbols.

$p_t \sim Q_s$, then $(dE/L^2)/d\eta = c'(N_c^2 - 1)Q_s^3/4\pi^2\alpha_S N_c$ which is of the same form as our Eq. (2). In the $g^2\mu L$ region of interest, our function $f \approx 0.23$–0.26. Using the relation between Q_s and $g^2\mu$ [11], we obtain $c' = 4.3$–4.9. It is very likely that c' is at least a factor of 2 greater than c. The latter will be determined more precisely when we compute the nonperturbative number and energy distributions.

We will now estimate the initial energy per unit rapidity of produced gluons at RHIC and LHC energies. We do so by extrapolating from our SU(2) results to SU(3) assuming the N_c dependence to be $(N_c^2 - 1)/N_c$ as in Mueller's formula. At late times, the energy density is $\varepsilon = (g^2\mu)^4 f(g^2\mu L)\gamma(g^2\mu L)/g^2$, where the formation time is $\tau_D = [1/\gamma(g^2\mu L)]/g^2\mu$ as discussed earlier. We find that $\varepsilon^{\mathrm{RHIC}} \approx 66.5\ \mathrm{GeV/fm}^3$ and $\varepsilon^{\mathrm{LHC}} \approx 1300\ \mathrm{GeV/fm}^3$. Multiplying these numbers by the initial volumes at the formation time τ_D, we obtain the classical Yang-Mills estimate for the initial energies per unit rapidity E_T to be $E_T^{\mathrm{RHIC}} \approx 2700$ GeV and $E_T^{\mathrm{LHC}} \approx 25\,000$ GeV, respectively.

Compare these numbers to results presented recently by Kajantie [26] for the minijet energy (computed for $p_t > p_{\mathrm{sat}}$, where p_{sat} is a saturation scale akin to Q_s). He obtains $E_T^{\mathrm{RHIC}} = 2500$ GeV and $E_T^{\mathrm{LHC}} = 12\,000$. The remarkable closeness between our results for RHIC is very likely a coincidence. Kajantie's result includes a K factor of 1.5—estimates range from 1.5–2.5 [27]. If we pick a recent value of $K \approx 2$ [28], we obtain as our final estimate $E_T^{\mathrm{RHIC}} \approx 5400$ GeV and $E_T^{\mathrm{LHC}} \approx 50\,000$ GeV.

In summary, we performed a nonperturbative, numerical computation, for a SU(2) gauge theory, of the initial energy, per unit rapidity, of gluons produced in very-high-energy nuclear collisions. Extrapolating our results to SU(3), we estimated the initial energy per unit rapidity at RHIC and LHC. We plan to improve our estimates by performing our numerical analysis for SU(3). Moreover, computations are in progress to determine the energy and number distributions [24].

We thank Dr. Frank Paige and Dr. Efstratios Efstathiadis for help with the BNL CCD Linux cluster. R. V. was supported at BNL under DOE Contract No. DE-AC02-98CH10886. A. K. acknowledges the support of the Portuguese Fundação para a Ciência e a Technologia, Grant No. CERN/P/FIS/1203/98. A. K. is grateful to the BNL Physics Department for hospitality during the course of this work. R. V. would like to thank Larry McLerran and Al Mueller for useful discussions.

[1] See, for instance, *Proceedings of Quark Matter 97, Tsukuba, Japan* [Nucl. Phys. **A638**, 329 (1998)].
[2] K. Kajantie, P. V. Landshoff, and J. Lindfors, Phys. Rev. Lett. **59**, 2527 (1987); K. J. Eskola, K. Kajantie, and J. Lindfors, Nucl. Phys. **B323**, 37 (1989); J.-P. Blaizot and A. H. Mueller, Nucl. Phys. **B289**, 847 (1987).
[3] X.-N. Wang, Phys. Rep. **280**, 287 (1997); K. Geiger, Phys. Rep. **258**, 237 (1995); B. Zhang, Comput. Phys. Commun. **104**, 70 (1997).
[4] K. J. Eskola, B. Müller, and X.-N. Wang, nucl-th/9608013; Phys. Lett. B **374**, 20 (1996).
[5] A. H. Mueller, Nucl. Phys. **B558**, 285 (1999); R. Venugopalan, hep-ph/9907209.
[6] L. McLerran and R. Venugopalan, Phys. Rev. D **49**, 2233 (1994); **49**, 3352 (1994); **50**, 2225 (1994).
[7] J. Jalilian-Marian, A. Kovner, L. McLerran, and H. Weigert, Phys. Rev. D **55**, 5414 (1997).
[8] J. Jalilian-Marian, A. Kovner, A. Leonidov, and H. Weigert, Nucl. Phys. **B504**, 415 (1997); Phys. Rev. D **59**, 034007 (1999); **59**, 099903 (1999); J. Jalilian-Marian, A. Kovner, and H. Weigert, Phys. Rev. D **59**, 014015 (1999); L. McLerran and R. Venugopalan, Phys. Rev. D **59**, 094002 (1999).
[9] M. Gyulassy and L. McLerran, Phys. Rev. C **56**, 2219 (1997).
[10] Yu. V. Kovchegov, Phys. Rev. D **54**, 5463 (1996); **55**, 5445 (1997).
[11] See Ref. [5] for a discussion. Also, if $Q_s \sim 1$ GeV for RHIC, $Q_s \sim \kappa\alpha_S\mu$ with $\kappa \sim 6$.
[12] A. Kovner, L. McLerran, and H. Weigert, Phys. Rev. D **52**, 3809 (1995); **52**, 6231 (1995).
[13] I. Balitsky, Phys. Rev. D **60**, 014020 (1999).
[14] Y. V. Kovchegov and D. H. Rischke, Phys. Rev. C **56**, 1084 (1997); S. G. Matinyan, B. Müller, and D. H. Rischke, Phys. Rev. C **56**, 2191 (1997); Phys. Rev. C **57**, 1927 (1998); Xiao-feng Guo, Phys. Rev. D **59**, 094017 (1999).
[15] J. F. Gunion and G. Bertsch, Phys. Rev. D **25**, 746 (1982).
[16] A. Krasnitz and R. Venugopalan, hep-ph/9706329; hep-ph/9808332.
[17] A. Krasnitz and R. Venugopalan, Nucl. Phys. **B557**, 237 (1999).
[18] R. V. Gavai and R. Venugopalan, Phys. Rev. D **54**, 5795 (1996).
[19] These considerations also apply to noncentral collisions of identical nuclei, and can be easily generalized to study nuclei with unequal A.
[20] J. D. Bjorken, Phys. Rev. D **27**, 140 (1983).
[21] In general, $\varepsilon\tau$ has the physical interpretation of an energy only at asymptotic τ. It converges to a constant value at a finite τ, and the rate of convergence is controlled by τ_D.
[22] The central values of γ are from uncorrelated fits to the $g^2\mu\tau$ history of $\varepsilon\tau/(g^2\mu)^3$. The errors on γ were qualitatively estimated by multiplying the naive errors from the uncorrelated fit by the square root of the number of degrees of freedom. A more rigorous correlated fit analysis cannot be reliably performed with our current relatively small data samples.
[23] Y. V. Kovchegov and A. H. Mueller, Nucl. Phys. **B529**, 451 (1998).
[24] A. Krasnitz and R. Venugopalan (to be published).
[25] A. H. Mueller, hep-ph/9906322.
[26] K. Kajantie, hep-ph/9907544.
[27] K. J. Eskola and K. Kajantie, Z. Phys. C **75**, 515 (1997).
[28] A. Leonidov and D. Ostrovsky, hep-ph/9811417.